Dysfunction of EAAT3 Enhances LPS-induced Postoperative Cognitive Dysfunction

Xiaoyan Wang
Departmemt of anesthesiology, the fourth Medical Center of PLA General Hospital
Yulong Ma
Department of anesthesiology, the first medical center of Chinese PLA general hospital
Aisheng Hou
Department of anesthesiology, the first medical center of Chinese PLA general hospital
Yuxiang Song
Department of anesthesiology, the first medical center of Chinese PLA general hospital
Xin Sui
Academy of Military Medical Sciences Institute of Pharmacology and Toxicology
Wengang Liu
Medical School of Chinese PLA: Chinese PLA General Hospital
Min Liu
Medical School of Nanjing University: Nanjing University Medical School
Yongan Wang
Academy of Military Medical Sciences Institute of Pharmacology and Toxicology
Jiangbei Cao (cjb2000@sina.com)
First Medical Center of Chinese PLA General Hospital https://orcid.org/0000-0003-1218-4639
Weidong Mi
department of Anesthesiology, the first medical center of Chinese PLA general hospital

Research

Keywords: Excitatory amino acid transporter 3 (EAAT3), Postoperative cognitive dysfunction (POCD), Lipopolysaccharide (LPS), riluzole, Aging

Posted Date: February 5th, 2021

DOI: https://doi.org/10.21203/rs.3.rs-141076/v2

Abstract

Background: Studies have shown that excitatory amino acid transporter 3 (EAAT3) function inhibition is related to several neurodegenerative diseases. Our previous studies also found that the EAAT3 function is intimately linked to learning and memory. In this study, we examined the role of EAAT3 in postoperative cognitive dysfunction (POCD) and explored the potential benefit of riluzole against POCD.

Methods: We measured EAAT3 protein expression in hippocampus of male mice at different ages. Next, we established a recombinant adeno-associated viral (rAAV)-mediated shRNA to knockdown EAAT3 expression in the hippocampus of adult male mice. And then the mice received 2μg of lipopolysaccharide (LPS) intracerebroventricular microinjection to construct the POCD model. In addition, we intraperitoneally injected 4mg/kg of riluzole 2 days before LPS microinjection for consecutive 3 days in elderly male mice. Cognitive function was assessed using a Morris water maze 24h after LPS microinjection. Animal behavioral tests, as well as pathological and biochemical assays, were performed to clarify the role of EAAT3 function in POCD and evaluate the effect of activation of EAAT3 function by riluzole.

Results: We found that the expression of EAAT3 was significantly decreased in old mice and EAAT3 knockdown in hippocampus aggravated LPS-induced learning and memory deficits in adult male mice. LPS significantly inhibited hippocampal EAAT3 membrane protein expression and GluA1 protein phosphorylation level in adult male mice. Moreover, riluzole pretreatment significantly increased hippocampal EAAT3 membrane protein expression and ameliorated LPS-induced cognitive impairment in old male mice.

Conclusions: Our results demonstrated that the dysfunction of EAAT3 is an important risk factor for POCD susceptibility and riluzole may be a promising strategy for prevention and treating of POCD in the elderly people.

Background

Postoperative cognitive dysfunction (POCD) is a postoperative complication of the central nervous system (CNS) that occurs mainly in elderly patients [1, 2]. It is characterized by anxiety, personality changes, and impaired memory. POCD can significantly affect postoperative recovery, increase morbidity and mortality rates as well as hospital expenses [3]. Moreover, with significant increases in life expectancy, and the demands for surgery in elderly patients, the health and economic burden caused by POCD have been on the rise. Although there are many basic and clinical studies on POCD, the reason for the susceptibility of POCD in elderly patients has yet not been identified.

Many preclinical and human studies have shown that neuroinflammation has an important role in the progression of POCD [2, 4]. Lipopolysaccharide (LPS) is a major bacterial TLR4 ligand that can activate innate immunity and induce inflammatory response [5]. Mounting evidence has shown that intracerebroventricular administration of LPS can be effectively used to establish a POCD model in mice [6–8].

Excitatory amino acid transporter 3 (EAAT3), also known as excitatory amino acid carrier 1 (EAAC1), is part of a family of Na^+-dependent excitatory amino acid transporters (EAATs) that regulate extracellular Glu homeostasis in the CNS [9, 10]. EAAT3 is encoded by the SLC1A1 gene, which ubiquitously exists in the brain and is enriched in the neurons of hippocampus and cortex [11, 12]. Previous studies have suggested that defective EAAT3 may lead to neuropsychiatric diseases such as Alzheimer's disease (AD), Parkinson's disease (PD), amyotrophic lateral sclerosis (ALS), Huntington's disease, epilepsy, and schizophrenia [13–18]. Evidence has also shown that loss of function SLC1A1 mutations cause human dicarboxylic aminoaciduria and, in some patients, mental retardation [19]. However, the relationship between EAAT3 activity and POCD has not been characterized.

Riluzole (2-amino-6-(trifluoromethoxy) benzothiazole) is a glutamate transporter activator [20], and an FDA approved drug for ALS treatment. Riluzole has also been recommended for the treatment of other neurodegenerative diseases, such as AD and Parkinson's disease [20, 21] and psychiatric disorders [22, 23]. Previous studies have also shown that riluzole can improve learning and memory function in aged and Alzheimer's disease rats [24]. However, whether riluzole can alleviate LPS-induced POCD in aged mice and its underlying molecular mechanism have not been reported so far.

In this study, we constructed a recombinant adeno-associated viral (rAAV) -mediated shRNA to knockdown EAAT3 expression in adult mice and established LPS-mediated cognitive impairment (POCD animal model) to identify the role of EAAT3 in POCD and its underlying mechanisms. We also explored whether riluzole could improve LPS-induced cognitive impairment in elderly mice. The results obtained in this study may provide new insights into the potential mechanisms for the prevention and treatment of POCD.

Materials And Methods

1. Animals

Adult (3months, weighing 22-25g) and aged (21months, weighing 28-36g male C57BL/6 mice were obtained from Beijing SPF Animal Technology Company (Beijing, China). Animals were housed in a temperature- and humidity-controlled room, 2-4 mice per cage, with a standard 12–12 light/dark cycle. They were fed food and water ad libitum. All animals were acclimatized to the environment for one week before the experiment and were fixed cage mates throughout the acclimation and testing periods. Each experimental group consisted of 5-12 mice, and mice in the same cage were in the same treatment group. The experimental animal procedures were approved by the Animal Care Committee of the Chinese People's Liberation Army General Hospital (Beijing, China). All animal experiments were carried out in accordance with the current laws of China and the National Institutes of Health Guide for the Care and Use of Laboratory Animals.

2. Drugs

The artificial cerebrospinal fluid (ACSF) vehicle contained 140 mM NaCl, 3.0 mM KCl, 2.5 mM $CaCl_2$, 1.0 mM $MgCl_2$, and 1.2 mM Na_2HPO_4. LPS (Sigma, St. Louis, MO, USA) was dissolved in ACSF (1000ng/mL).

Riluzole (Cayman Chemical Company, USA) was first dissolved in dimethylsulphoxide (DMSO; Fish Scientific, NJ) to 100 mM (27 mg/ml) and then diluted in saline to 0.4 mg/ml with gentle warming. It (4 mg/kg) was then intraperitoneally injected 2h before Morris Water Maze (MWM) acquisition training or LPS microinjection. The same concentration of DMSO (1.6%) was used as solvent control.

3. Experimental design and groups

The experiments were carried out between 8:00 am and 6:00 pm. All mice were sacrificed by deep sodium pentobarbital anesthesia (100 mg/kg) for obtaining the tissue. The following sets of experiments were performed.

Experiment 1: Detection EAAT3 expression in the hippocampus of adult and aged mice

Six adult and six aged mice were randomly selected as Adult and Old groups. Animals were decapitated, and their hippocampi were removed for western blot analysis.

Experiment 2: The establishment of mice with hippocampus EAAT3 knockdown

Recombinant adeno-associated viral (rAAV) vectors were microinjected into the mouse hippocampus by stereotactic technique to construct the hippocampal EAAT3 knockdown model. After receiving bilateral hippocampal microinjection of RNA interference vector (RNAi), 36 adult mice were randomly divided into six groups (n=6 for each): CON (immediately after microinjection, Day 0), D1, D7, D14, D21, and D28. The mice were used to obtain hippocampal tissue for RT-qPCR and Western blot analysis.

Twenty adult mice were randomly separated into two groups according to receiving rAAV-shRNA-NC (NC) or rAAV-shRNA-mSLC1A1 (RNAi) (n=10): NC group, and RNAi group. The spontaneous activities of mice were observed by an Open field test (OFT) 21 days after microinjection in the hippocampus. Five mice in each group were randomly selected to perform brain immunofluorescence after OFT.

Experiment 3: Effect of LPS on hippocampal EAAT3 knockdown mice and mechanism

Adult mice were randomly assigned to four groups according to whether they received rAAV-shRNA-NC (NC), rAAV-shRNA-mSLC1A1 (RNAi), ACSF/LPS (n=12): NC+ACSF group, NC+LPS group, RNAi+ACSF

group, and RNAi+LPS group.

Sixteen days after microinjection in the hippocampus, four groups of mice received MWM training for 5 days. Twenty-one days after microinjection in hippocampus, all mice received intracerebroventricular microinjection of ACSF or LPS. After 24h, mice were subjected to the MWM probe test. Six mice in each group were used for harvesting the hippocampus for western blot analysis; in other mice brain tissues were dissected for Golgi-Cox Staining after the behavioral observation.

Experiment 4: Effect of Riluzole on LPS-induced cognitive impairment in the old mice

The old mice were randomly divided into four groups according to whether they received DMSO, Riluzole, or LPS treatment (n=8 in each group): Old+DMSO, Old+Riluzole, Old+DMSO+LPS, and Old+Riluzole+LPS. The mice in Old+DMSO+LPS and Old+Riluzole+LPS received an intraperitoneal injection of DMSO or Riluzole 2 days before LPS microinjection for consecutive 3 days. The probe test for reference memory was conducted 1 day after LPS administration, and the hippocampus was obtained for western blot analysis after the test.

4. Construction of hippocampal EAAT3 knockdown mouse model mediated by shRNA

Four potential different shRNA sequences (shRNA-mSLC1A1-1～4) targeting mSLC1A1 and the negative control shRNA (shRNA-NC) were designed and synthesized to construct rAAV vectors respectively named rAAV-shRNA-SLC1A1-1～4 and rAAV-shRNA-NC by Gemma Gene Company (Suzhou, China). To identify the most effective shRNA sequence that could knockdown EAAT3 in the hippocampus, we screened 4 different sequences to infect the HT-22 cell line, finding that rAAV-shRNA-SLC1A1-2 displayed the lowest EAAT3 expression level by RT/PCR and western blot (Suppl. Fig. 1).

For stereotactic injection of rAAV vector into the bilateral hippocampus, mice were anesthetized with pentobarbital sodium (70mg/kg) and placed on brain stereotaxic apparatus (RWD Life Science, Shenzhen, China). After exposing the skull via an incision, two small holes were drilled for injection. The stereotactic coordinates were 2.1 posterior, ± 1.7 lateral, and 2.0 ventral from bregma. Injection speed was 50nl/min, and the needle was kept in place for an additional 15 minutes before it was slowly withdrawn. RNAi group and RNAi+LPS group received bilateral hippocampal microinjection of rAAV-RNAi at 1μL per side (1×10^{13}TU/mL), while the NC group and NC+LPS group received an equal volume of negative control rAAV-NC.

5. Open field test

To evaluate the effects of hippocampal injection of rAAV-RNAi on spontaneous activity in mice, an open field test was carried out 21 days after bilateral hippocampal rAAV-RNAi injection. Mice were placed in the corner of an opaque plastic box (50×50×30cm) in which the base was equally divided into 16 parts (4×4). A camera was set up right above the box to record all the activities of the mice. The parameters such as total moving distance, moving speed, and times of grid crossing were recorded for 5 min and analyzed by the ANY-MAZE system. The open field was cleaned with 5% ethyl alcohol and allowed to dry between tests.

6. Establishment of LPS-induced cognitive impairment model

The LPS-induced cognitive impairment mouse model was performed according to the previously described protocol [7]. LPS was administered via the intracerebroventricular (i.c.v.) route; the stereotactic coordinates were 0.5 posterior, ± 1.0 lateral, and 2.0 ventral from bregma. After anesthesia with pentobarbital sodium (65-70 mg/kg ip), mice received 2μL LPS microinjection.

7. MWM test

The MWM test, a hippocampal-dependent test of spatial learning and memory for rodents, was performed as previously described [25] with minor modifications. The water maze was a stainless steel circular pool (diameter 125cm, high 50cm) with a white inner wall, filled with opaque water containing skimmed milk powder at 22 ± 1.0 ℃ (water depth 25cm).

The pool with automatic visual tracking cameras on the ceiling can record the whereabouts of mice. The pool was divided into four equal quadrants Ⅰ, Ⅱ, Ⅲ, and Ⅳ. An escape platform (diameter 10cm) fixed in the first quadrant (target quadrant) was submerged below the water surface 1cm. The spatial learning was evaluated through a 5-day repetitive trial. Mice were randomly released into the pool facing the wall and trained to find the platform within 60s. When the mouse failed to find the platform, it was guided to it. All mice were given four trials (once per quadrant; swim-start position randomized) each day and were allowed to stay on the platform for 10s. After the daily session, mice were dried under a heater and returned to the home cage.

Animals underwent LPS microinjection 24 h after the final acquisition trial, and a probe trial was conducted by removing the hidden platform to assess spatial reference memory 24 h after the microinjection. Total swimming distance, average speed, platform-site crossings, the times of entering the target quadrant (original platform quadrant), and time in the target quadrant were recorded. Each mouse was placed in the pool for 60 s at a time, and the starting point of entry was the third quadrant (opposite to the first quadrant).

8. Real-time reverse transcription polymerase chain reaction (RT-qPCR)

Total cellular RNA samples from mouse hippocampus were extracted using the Trizol^{TM} Reagent (Invitrogen, USA). RT-PCR was performed using the ThermoScript RT-PCR System (Invitrogen). Primers used for amplifying SLC1A1 were: 5'- AAGAACCCTTTCCGCTTTG -3' (sense) and 5'- TTGCCGAACTGGACGAGA -3' (antisense); GAPDH primers were: 5'- CCTTCATTGACCTCAACTACATGG -3' (sense) and 5'- CTCGCTCCTGGAAGATGGTG -3' (antisense).

9. Western blot

The total protein and membrane protein were extracted from hippocampal tissue of the mice using a Whole Protein Extraction Kit (KGP250, KeyGEN, Nanjing, China) and a Membrane Protein and Cytoplasmic Protein Extraction Kit (KGP350, KeyGEN, Nanjing, China), respectively. The protein concentrations were then determined by BCA Protein Assay (KeyGEN, Nanjing, China). Equal amounts (30 μg) of proteins were separated by SDS-PAGE and transferred to a polyvinylidene fluoride membrane (Millipore, Billerica, MA, USA). The membrane was blocked with 5% skim milk for 2h at room temperature, then incubated overnight at 4°C with the following primary antibody: rabbit anti-EAAT3 (1:1,000; Cell Signaling Technology), rabbit anti-AMPA Receptor 1 (GluA1) (1:1,000; Cell Signaling Technology), rabbit anti-Phospho-GluA1-Ser845 (1:1,000; Cell Signaling Technology), rabbit anti-GAPDH (1:1000, Abcam) and rabbit anti-β-actin antibody (1:1000, Cell Signaling Technology). after which, it was washed three times (5 min each) in Tris-buffered saline-Tween 20 (TBST) buffer, incubated in the goat anti-rabbit horseradish peroxidase (HRP)-conjugated secondary antibody (1:2000 in TBST buffer) at room temperature for 1h, and washed again. The optical densities of each protein band were measured with ImageLab software (Bio-Rad). Each experiment was repeated at least four times. Relative expression levels of proteins were normalized to β-actin.

10. Fluorescence immunohistochemistry

The brain tissue of mice was fixed with 4% paraformaldehyde for 2 days and then embedded in paraffin. Coronal 3μm sections were prepared and stained with fluorescence immunohistochemistry. First, paraffin sections were dewaxed and placed in the EDTA buffer (pH8.0) to repair the antigen. Second, sections were washed in 0.01% Triton X-100 in phosphate-buffered saline (PBS-T) and blocked with 3% hydrogen peroxide for 15 min at room temperature. Then, samples were incubated overnight at 4℃ in the appropriate primary antibody, anti-EAAT3 (1:400; Cell Signaling Technology). Next, the sections were incubated with the appropriate fluorescent secondary antibody, anti-rabbit IgG (1:400; ZF-0513), for 30 min at 37℃. After washing out the secondary antibodies, sections were incubated with 4',6-diamidino-2-phenylindole (DAPI) for nuclear staining. Immunofluorescence was captured with a scanning confocal microscope.

11. Golgi-Cox Staining

The Golgi-Cox method is one of the most effective techniques for studying the morphology of neuronal dendrites and dendritic spines [26]. The brains of mice were quickly removed and rinsed with double distilled water and were stained with the FD Rapid Golgi Stain™ kit (FD Neuro Technologies, Ellicott City, MD, USA) according to manufacturer's instructions. Coronal slices (100 μm thickness) were obtained by using a cryostat (Leica, Wetzlar, Germany), and then were placed on a gelatin-coated microscope slide, stained and dehydrated. Images were taken by using an Eclipse Ci-L microscope (Nikon, Japan) and Image-Pro Plus 6.0 software. Sholl analyses were performed using the ImageJ 1.51K Sholl plugin. Spine density was estimated as the number of spines per 10 μm of dendrite length. The number of dendrites was estimated by counting dendritic intersections with multiple circular regions of interest centered on the cell soma with a spacing of 10 μm.

12. Statistical analysis

All data were analyzed by an observer who was blinded to the experimental protocol. Fisher exact probability method was used for descriptive analyses. Statistical comparisons between and within groups were made by two-way ANOVA, followed by a Tukey test where necessary. For acquisition training, data were analyzed using two-way ANOVA (treatment × trial time) with repeated measures (trial days) followed by the Bonferroni post hoc test. For all other data, two-way ANOVA was used. The results of behavioral counting were expressed as median (first quartile, third quartile), and the other results were expressed as mean ± standard error (SE); P values <0.05 were considered as statistically significant.

Results

1. Hippocampal EAAT3 protein expression was significantly decreased in old mice

To determine whether there was any difference in the expression of EAAT3 in the hippocampus of adult and old mice, we measured the expression of total protein and membrane protein in the hippocampus of mice in the Adult and Old group by western blot. The results showed that EAAT3 expression of total protein (Fig. 1A, $^{**}P < 0.01$) and membrane protein (Fig. 1B, $^{**}P < 0.01$) in the hippocampus of the Old group was significantly lower than that in the Adult group.

2. Expression of EAAT3 in adult mice hippocampus was significantly decreased 21 days after microinjection rAAV-RNAi targeting EAAT3

To verify the effect of RNAi mediated-knockdown of EAAT3 on adult mouse hippocampus, the hippocampus tissues were collected at different time points (0, 1, 7, 14, 21, and 28 days) after the microinjection of rAAV-RNAi for RT-qPCR and western blot analysis. The PCR results showed that the hippocampal EAAT3 mRNA expression was significantly decreased on Day 21 ($^{*}P < 0.05$) and Day 28 (*P < 0.05) compared with the CON group (Fig. 2B). Moreover, the western blot results showed that the hippocampal EAAT3 protein levels were significantly decreased on Day7 ($^{***}P<0.001$) and remained downregulated on Day14 ($^{**}P<0.01$), Day21 ($^{***}P<0.001$), and Day28 ($^{***}P<0.001$) compared with the CON group (Fig. 2C). In addition, the immunofluorescence results showed that the expression of EAAT3 in the hippocampal CA area of the RNAi group was significantly lower than that of the NC group after receiving hippocampal microinjection for 21 days (Fig. 2A).

3. EAAT3 knockdown in the hippocampus significantly increased the motility of adult mice

Twenty-one days after hippocampal microinjection of rAAV-RNAi/NC, adult mice's autonomic activity was examined by open field test. The results showed that the total moving distance ($^{**}P < 0.01$), moving speed ($^{*}P < 0.05$), and times of grid crossing

($^{*}P < 0.05$) in RNAi group were significantly higher than those in the NC group (Fig. 3).

4. EAAT3 knockdown in hippocampus significantly aggravated LPS-induced learning and memory deficit in adult mice

The MWM test was conducted to examine the effects of EAAT3 knockdown in the hippocampus on the LPS-induced learning and memory deficit model. In the MWM test, all adult animals learned the original platform location on the fourth day during the acquisition phase. The escape latency in all groups shortened as the training times increased ($^{**}P < 0.01$, $^{*}P < 0.05$); yet, no difference was observed between the groups on the same day (Fig. 4A). During the probe test, it was observed that the times of entering the target quadrant of mice in RNAi + ACSF group and NC + LPS group were significantly reduced compared with that in NC + ACSF group ($^{*}P < 0.05$), and that in RNAi + LPS group were lower than that in NC + LPS group ($^{\#}P < 0.05$)(Fig. 4B). Similarly, the platform-site crossings of mice in RNAi + ACSF group and NC + LPS group were significantly reduced compared with that in NC + ACSF group ($^{*}P < 0.05$), and the platform-site crossings of mice in RNAi + LPS group were lower than that in NC + LPS group ($^{\#}P < 0.05$) (Fig. 4C).

5. LPS significantly decreased EAAT3 plasma membrane protein level in the adult mice

To determine the effect of LPS on EAAT3 protein expression, western blot analyses were performed to detect both EAAT3 total protein levels and membrane protein levels in the hippocampus. As shown in Fig. 5A, we found that EAAT3 total protein level in RNAi + ACSF group was significantly lower than that in NC + ACSF group ($^{*}P < 0.05$), and that EAAT3 total protein level in RNAi + LPS group was also significantly lower than that in NC + LPS group ($^{\#}P < 0.05$). There is no significant difference regarding EAAT3 total protein level between the RNAi + ACSF group and RNAi + LPS group.

As shown in Fig. 5B, EAAT3 plasma membrane protein level in NC + LPS group was significantly lower than that in NC + ACSF group ($^{**}P < 0.01$), and EAAT3 plasma membrane protein level in RNAi + LPS group was significantly lower than that in NC + LPS group ($^{\#}P < 0.05$) and RNAi + ACSF group ($^{\&\&}P < 0.01$).

6. Expression of GluA1 proteins and GluA1 phosphorylation is inhibited by LPS in the hippocampus of EAAT3 knockdown mice

Next, we explored the effect of EAAT3 knockdown and LPS microinjection on GluA1 expression. As shown in Fig. 6A, the GluA1 total protein expression level in the RNAi + ACSF group was significantly decreased compared to that in the NC + ACSF group ($^{*}P < 0.05$), and the GluA1 total protein expression level in the RNAi + LPS group was significantly decreased compared to that in NC + LPS group ($^{\#}P < 0.05$).

As shown in Fig. 6B, the phosphorylation level of GluA1 protein at Serine 845 site (p-GluA1-Ser-845) in NC + LPS group was significantly lower than that in NC + ACSF group ($^{*}P < 0.05$), and p-GluA1-Ser-845 level in RNAi + LPS group was significantly lower than that in NC + LPS group ($^{\#}P < 0.05$) and RNAi + ACSF group ($^{\&}P < 0.05$).

7. Effects of LPS on neuronal dendritic morphology in hippocampus of EAAT3 knockdown mice

To investigate the effect of EAAT3 knockdown and LPS microinjection on neuronal dendritic morphology, we measured the density of dendritic spines and dendritic branch numbers of the hippocampus one day after LPS intracerebroventricular injection. As shown in Fig. 7A, the densities of dendritic spines were markedly decreased in the NC + LPS group ($^{***}P < 0.001$) and RNAi + ACSF group ($^{*}P < 0.05$) compared with that in the NC + ACSF group, and that in the RNAi + LPS group was significantly lower than that in NC + LPS group ($^{\#}P < 0.05$) and RNAi + ACSF group ($^{\&\&\&}P < 0.001$).

As shown in Fig. 7B, the number of intersections between dendritic processes and ten concentric circles centered on the cell soma with a spacing of 10μm were counted to estimate the number of dendrites. We found that the number of intersections in the NC + LPS group was significantly decreased compared to that in the NC + ACSF group ($^{*}P < 0.05$), and the number of intersections in the RNAi + LPS group was significantly decreased compared to that in the NC + LPS group ($^{\#}P < 0.05$) and RNAi + ACSF group ($^{\&}P < 0.05$).

8. Riluzole improves learning and memory ability and LPS-induced cognitive impairment in old mice

Finally, we explored whether riluzole could improve the cognitive deficits induced by LPS in old mice. Regarding the MWM test, during the training phase, all old mice were able to learn the original platform location on the fourth day, and the escape latency in all groups shortened as the training times increased compared with the first day ($^{*}P < 0.05$); yet, no difference was observed between the Old + DMSO group and Old + Riluzole group on the same day (Fig. 8A). During the probe test, it was observed that compared with the Old + DMSO group, the time in the target quadrant of mice in the Old + Riluzole group was significantly increased ($^{*}P < 0.05$), whereas the time in the target quadrant of mice in the Old + DMSO + LPS group was significantly decreased ($^{*}P < 0.05$). In addition, the time in the target quadrant of mice in the Old + Riluzole + LPS group was significantly decreased compared with that in the Old + DMSO + LPS group ($^{\#}P < 0.05$)(Fig. 8B). Similarly, compared with the Old + DMSO group, the platform-site crossings of mice in the Old + Riluzole group were significantly increased ($^{*}P < 0.05$), whereas the platform-site crossings of mice in the Old + DMSO + LPS group were significantly decreased ($^{*}P < 0.05$). Also, the platform-site crossings of mice in the Old + Riluzole + LPS group were significantly less than that in the Old + DMSO + LPS group ($^{\#}P < 0.05$)(Fig. 8C).

9. Riluzole significantly increased EAAT3 membrane protein level in the hippocampus of the old mice

To explore a potential mechanism for riluzole treatment, improving learning and memory in old mice, we investigated the effect of riluzole on the expression levels of EAAT3 in the hippocampus by western blot. For EAAT3 total protein expression, there was no significant difference among different groups (Fig. 9A). Yet, EAAT3 plasma membrane protein expression in the Old + Riluzole group was significantly increased compared with that in the Old + DMSO group ($^{*}P < 0.05$). Moreover, the EAAT3 plasma membrane protein expression in the Old + DMSO + LPS group was significantly decreased compared with that in the Old + DMSO group ($^{*}P < 0.05$), and EAAT3 plasma membrane protein expression in the Old + Riluzole + LPS group was significantly lower than that in the Old + Riluzole group ($^{\#}P < 0.05$)(Fig. 9B).

Discussion

Postoperative cognitive dysfunction (POCD) is commonly observed in perioperative care following surgery and general anesthesia in elderly individuals. Yet, its underlying mechanisms remain largely unknown. In addition, no preventive or interventional agents have been established so far. Previous studies suggested that extracellular glutamate increased in the brain with age and that its dysregulation is associated with impaired learning and memory [27–29].

EAAT3 is part of a family of Na^+-dependent excitatory amino acid transporters that regulate extracellular glutamate homeostasis in the CNS, which is encoded by the SLC1A1 gene and is enriched in the hippocampus neurons [11, 12].. EAAT3 has been found to play a critical role in learning and memory [30]. And previously, we found that lack of EAAT3 effects leads to impaired cognition after isoflurane exposure in EAAT3(-/-) mice [31]. Accordingly, we detected EAAT3 expression in adult and old mice. Our results revealed that both expressions of EAAT3 total protein and membrane protein in the old mice hippocampus were significantly decreased compared to the adult mice. Combining with the higher incidence of POCD in the elderly, we inferred that the dysfunction and degradation of EAAT3 expression increased the susceptibility to POCD in the elderly. However, the underlying mechanism is still elusive.

Previous studies have used the EAAT3 gene knockout animal model to explore the function of EAAT3 in the CNS [32–34]. Considering that the animal models with reduced gene expression rather than deletion are of clinical relevance since they better reflect the impact of human polymorphisms affecting protein levels and rarely complete loss of expression [35], in this study, we constructed rAAV-mediated shRNA to knockdown hippocampal EAAT3 expression via hippocampal microinjection, which achieved the local interference and minimized the impact on the whole brain and the whole body [36]. The results of RT-qPCR and western blot confirmed that bilateral hippocampal injection of RNAi could significantly inhibit hippocampal EAAT3 expression and achieve a stable knockdown effect from 21 to 28 days after RNAi injection, which is consistent with the time point selected by other AAV vectors injection studies [37, 38]. Also, we found that the autonomic activity (including total moving distance, moving speed, and times of grid crossing) in the RNAi group was significantly higher than those in the NC group, which may be due to the increased glutamate between synaptic space induced by the interference of EAAT3 expression.

Glutamate acts as the major excitatory neurotransmitter and mediates fast neurotransmission in neuronal networks [39]. The interference of EAAT3 expression can disrupt the absorption of extracellular glutamate (Glu) and lead to neuronal hyperexcitation and excitotoxicity injury [40]. These results indicated that the interference of EAAT3 expression could increase extracellular glutamate level and finally, brain excitability. However, the role of EAAT3 in POCD has been rarely explored.

We used the intracerebroventricular administration of LPS to construct the POCD model according to our previously described approach [7]. Our results revealed that LPS led to significant learning and memory deficits detected by the MWM task and that interference of EAAT3 expression by rAAV-RNAi significantly aggravated the learning and memory impairment induced by LPS. These results indicated that EAAT3

dysfunction increased the susceptibility to LPS-mediated learning and memory deficits. However, the underlying mechanism is still elusive.

Under basal conditions, EAAT3 is primarily sequestered in the intracellular compartment, with about 20% of the transporter localized at the cell surface [41], which is a key determinant of its buffering efficiency [42] and accounts for 40% of glutamate uptake in the hippocampus [10]. In this study, we found that LPS treatment did not significantly decrease the EAAT3 total protein level ether in NC group or in RNAi group but significantly decreased the EAAT3 plasma membrane protein level both in NC group and in RNAi group, thus indicating that LPS mainly disrupted the expression of EAAT3 plasma membrane protein. Interestingly, we also found that, in ACSF group, rAAV-RNAi only significantly decreased EAAT3 total protein level, but did not significantly decrease EAAT3 membrane protein level; however, in LPS treatment group, rAAV-RNAi significantly decreased both EAAT3 total protein level and EAAT3 membrane protein level, which further demonstrated that LPS primarily disrupted EAAT3 plasma membrane protein. So far, no study has reported this finding. Yet, the expression of SLC1A1, encoding EAAT3, is impaired in diseases related to neuroinflammation, such as multiple sclerosis, schizophrenia, hypoxia/ischemia, and epilepsy [43], which suggests that neuroinflammation induced by LPS maybe lead to the disruption of EAAT3 plasma membrane protein. However, the underlying mechanisms need to be further explored.

Trafficking of AMPAR to the plasma membrane in the neurons is believed to be a fundamental cellular process for learning and memory [44–46], mediated via the phosphorylation of GluA1 (an AMPAR subunit) at serine 845 (P-GluA1-s845) and then promoting AMPAR trafficking to the plasma membrane [45–47]. In this study, we found that LPS treatment did not significantly decrease the GluA1 protein level in the NC group or in the RNAi group, while it significantly decreased the P-GluA1-s845 level, which indicated that LPS primarily interfered with the P-GluA1-s845 level. In addition, we found that interference of EAAT3 expression by rAAV-RNAi significantly decreased both the GluA1 protein level and the P-GluA1-s845 level, thus indicating that EAAT3 could affect the expression of GluA1 and P-GluA1-s845. Moreover, our previous research also found that EAAT3 could regulate GluA1 trafficking to the plasma membrane [48]. These results indicated that LPS disrupted the P-GluA1-s845 by interfering with EAAT3 expression, and EAAT3 may become a new therapeutic target for POCD.

Dendritic spines, defined as small protrusions arising from dendrites, are used for communication by excitatory glutamatergic synapses of the CNS. They are remarkably dynamic structures that may undergo adaptive changes following different stimuli [49], and their structural plasticity is thought to underlie memory formation [50]. In this study, we found that LPS treatment significantly decreased the densities of dendritic spines and dendritic processes intersections. Many studies have shown that LPS could significantly reduce the dendritic spine density in hippocampal neurons [51, 52] by activating microglia to hyperactively secret proinflammatory cytokines [53]. In addition, glutamate excitotoxicity, which could be induced by the interference of EAAT3 expression, is a mechanism that causes secondary damage to neurons, accompanied by loss of dendritic spines and changes of synaptic activity [54, 55]. Our data indicated that interference of EAAT3 expression significantly decreased the dendritic spine density, and

LPS treatment further aggravated this impairment. Thus, we inferred that LPS decreased the dendritic spine density by interfering with EAAT3 expression.

Previous studies have indicated that riluzole is beneficial for neurodegenerative diseases such as AD [24] and PD [22, 23]. In this study, we found that, in old mice, riluzole pretreatment significantly promoted their learning and memory function and increased the EAAT3 membrane protein level, but not EAAT3 total protein level. This demonstrated that the riluzole could improve the cognitive function of old animals by promoting EAAT3 membrane protein level. In LPS treated old mice, riluzole pretreatment significantly alleviated LPS induced learning and memory deficits, which may be related to its up-regulation effect of EAAT3 membrane protein level. However, riluzole did not promote EAAT3 membrane protein level in LPS treated old mice, which may be due to the serious disruption of LPS on EAAT3 membrane protein in old mice. Thus, riluzole could be identified as a new strategy for POCD prevention in old surgery patients.

In conclusion, this study showed that the decrease of EAAT3 expression and function is associated with advanced age, and the decrease of EAAT3 expression can aggravate the cognitive impairment induced by LPS. Inflammation-induced by LPS significantly decreases the plasma membrane expression of EAAT3 in the hippocampus, which in turn inhibits the phosphorylation of Glua1, the mechanism of AMPAR transport to the plasma membrane, and reduces synaptic density in hippocampal neurons. This may be the reason why EAAT3 knockdown aggravates the cognitive impairment induced by LPS.

Abbreviations

POCD: Postoperative cognitive dysfunction; EAATs: Excitatory amino acid transporters; EAAT3: Excitatory amino acid transporter 3; Glu: Glutamate; AD: Alzheimer's disease; PD: Parkinson's disease; ALS: amyotrophic lateral sclerosis; LPS: lipopolysaccharide; CNS: central nervous system; rAAV: Recombinant adeno-associated viral; ACSF: Artificial cerebrospinal fluid; DMSO: dimethylsulphoxide; RNAi: RNA interference vector; OFT: Open field test; MWM: Morris Water Maze; TBST: Tris-buffered saline-Tween 20; HRP: anti-rabbit horseradish peroxidase; RT-qPCR: Real-time reverse transcription polymerase chain reaction; PBS-T: phosphate-buffered saline; DAPI: 4',6-diamidino-2-phenylindole SE: standard error

Declarations

Acknowledgements

Not applicable

Authors' contributions

XY Wang, YL Ma, and AS Hou conducted most of the experiments and drafted the manuscript. WG Liu and M Liu contributed to the statistical analysis and manuscript editing. YX Song, X Sui, and YA Wang

contributed to data interruption. JB Cao and WD Mi designed this study and edited the manuscript. All authors read and approved the final manuscript.

Funding

This work was supported by the National Natural Science Foundation of China (grant numbers 81771129, 81801138, 81671039). The funding sources had no contribution to the study design, collection, analysis, interpretation of the data, or writing of the report for publication.

Availability of data and materials

The datasets during and/or analyzed during the current study are available from the corresponding author on reasonable request.

Ethics approval and consent to participate

The experimentation procedures were approved by the Animal Care Committee of Chinese PLA General Hospital (Beijing, China). The maintenance and handling of the mice were consistent with the guidelines of the National Institutes of Health, and adequate measures were taken to minimize animal discomfort.

Consent for publication

Not applicable.

Competing interests

The authors declare that they have no known competing financial interests or personal relationships that could have appeared to influence the work reported in this paper.

References

1. Benson RA, Ozdemir BA, Matthews D, Loftus IM. A systematic review of postoperative cognitive decline following open and endovascular aortic aneurysm surgery. Annals of the Royal College of Surgeons of England. 2017;99(2):97-100.
2. Safavynia SA, Goldstein PA. The Role of Neuroinflammation in Postoperative Cognitive Dysfunction: Moving From Hypothesis to Treatment. Frontiers in psychiatry. 2018;9:752.
3. Xu Z, Dong Y, Wang H, Culley DJ, Marcantonio ER, Crosby G, et al. Age-dependent postoperative cognitive impairment and Alzheimer-related neuropathology in mice. Scientific reports. 2014;4:3766.

4. Shi C, Yi D, Li Z, Zhou Y, Cao Y, Sun Y, et al. Anti-RAGE antibody attenuates isoflurane-induced cognitive dysfunction in aged rats. Behavioural brain research. 2017;322(Pt A):167-176.
5. Banoub JH, El Aneed A, Cohen AM, Joly N. Structural investigation of bacterial lipopolysaccharides by mass spectrometry and tandem mass spectrometry. Mass spectrometry reviews. 2010;29(4):606-650.
6. Bossù P, Cutuli D, Palladino I, Caporali P, Angelucci F, Laricchiuta D, et al. A single intraperitoneal injection of endotoxin in rats induces long-lasting modifications in behavior and brain protein levels of TNF-α and IL-18. Journal of neuroinflammation. 2012;9:101.
7. Zhang XY, Cao JB, Zhang LM, Li YF, Mi WD. Deferoxamine attenuates lipopolysaccharide-induced neuroinflammation and memory impairment in mice. Journal of neuroinflammation. 2015;12:20.
8. Zhao WX, Zhang JH, Cao JB, Wang W, Wang DX, Zhang XY, et al. Acetaminophen attenuates lipopolysaccharide-induced cognitive impairment through antioxidant activity. Journal of neuroinflammation. 2017;14(1):17.
9. Bjørn-Yoshimoto WE, Underhill SM. The importance of the excitatory amino acid transporter 3 (EAAT3). Neurochemistry international. 2016;98:4-18.
10. Sheldon AL, González MI, Robinson MB. A carboxyl-terminal determinant of the neuronal glutamate transporter, EAAC1, is required for platelet-derived growth factor-dependent trafficking. The Journal of biological chemistry. 2006;281(8):4876-4886.
11. Rothstein JD, Martin L, Levey AI, Dykes-Hoberg M, Jin L, Wu D, et al. Localization of neuronal and glial glutamate transporters. Neuron. 1994;13(3):713-725.
12. Sims KD, Straff DJ, Robinson MB. Platelet-derived growth factor rapidly increases activity and cell surface expression of the EAAC1 subtype of glutamate transporter through activation of phosphatidylinositol 3-kinase. The Journal of biological chemistry. 2000;275(7):5228-5237.
13. Hodgson N, Trivedi M, Muratore C, Li S, Deth R. Soluble oligomers of amyloid-β cause changes in redox state, DNA methylation, and gene transcription by inhibiting EAAT3 mediated cysteine uptake. Journal of Alzheimer's disease : JAD. 2013;36(1):197-209.
14. Duerson K, Woltjer RL, Mookherjee P, Leverenz JB, Montine TJ, Bird TD, et al. Detergent-insoluble EAAC1/EAAT3 aberrantly accumulates in hippocampal neurons of Alzheimer's disease patients. Brain pathology. 2009;19(2):267-278.
15. Lane MC, Jackson JG, Krizman EN, Rothstein JD, Porter BE, Robinson MB. Genetic deletion of the neuronal glutamate transporter, EAAC1, results in decreased neuronal death after pilocarpine-induced status epilepticus. Neurochemistry international. 2014;73:152-158.
16. Sala G, Beretta S, Ceresa C, Mattavelli L, Zoia C, Tremolizzo L, et al. Impairment of glutamate transport and increased vulnerability to oxidative stress in neuroblastoma SH-SY5Y cells expressing a Cu,Zn superoxide dismutase typical of familial amyotrophic lateral sclerosis. Neurochemistry international. 2005;46(3):227-234.
17. McCullumsmith RE, Meador-Woodruff JH. Striatal excitatory amino acid transporter transcript expression in schizophrenia, bipolar disorder, and major depressive disorder.

Neuropsychopharmacology. 2002;26(3):368-375.

18. Gil YS, Kim JH, Kim CH, Han JI, Zuo Z, Baik HJ. Gabapentin inhibits the activity of the rat excitatory glutamate transporter 3 expressed in Xenopus oocytes. European journal of pharmacology. 2015;762:112-117.
19. Bailey CG, Ryan RM, Thoeng AD, Ng C, King K, Vanslambrouck JM, et al. Loss-of-function mutations in the glutamate transporter SLC1A1 cause human dicarboxylic aminoaciduria. The Journal of clinical investigation. 2011;121(1):446-453.
20. Carbone M, Duty S, Rattray M. Riluzole neuroprotection in a Parkinson's disease model involves suppression of reactive astrocytosis but not GLT-1 regulation. BMC neuroscience. 2012;13:38.
21. Okamoto M, Gray JD, Larson CS, Kazim SF, Soya H, McEwen BS, et al. Riluzole reduces amyloid beta pathology, improves memory, and restores gene expression changes in a transgenic mouse model of early-onset Alzheimer's disease. Translational psychiatry. 2018;8(1):153.
22. Pittenger C, Coric V, Banasr M, Bloch M, Krystal JH, Sanacora G. Riluzole in the treatment of mood and anxiety disorders. CNS drugs. 2008;22(9):761-786.
23. Ohashi M, Saitoh A, Yamada M, Oka J, Yamada M. Riluzole in the prelimbic medial prefrontal cortex attenuates veratrine-induced anxiety-like behaviors in mice. Psychopharmacology. 2015;232(2):391-398.
24. Pereira AC, Gray JD, Kogan JF, Davidson RL, Rubin TG, Okamoto M, et al. Age and Alzheimer's disease gene expression profiles reversed by the glutamate modulator riluzole. Molecular psychiatry. 2017;22(2):296-305.
25. Vorhees CV, Williams MT. Morris water maze: procedures for assessing spatial and related forms of learning and memory. Nature protocols. 2006;1(2):848-858.
26. Du F. Golgi-Cox Staining of Neuronal Dendrites and Dendritic Spines With FD Rapid GolgiStain™ Kit. Current protocols in neuroscience. 2019;88(1):e69.
27. Donzanti BA, Hite JF, Yamamoto BK. Extracellular glutamate levels increase with age in the lateral striatum: potential involvement of presynaptic D-2 receptors. Synapse. 1993;13(4):376-382.
28. Massieu L, Tapia R. Glutamate uptake impairment and neuronal damage in young and aged rats in vivo. Journal of neurochemistry. 1997;69(3):1151-1160.
29. Brimson JM, Brimson SJ, Brimson CA, Rakkhitawatthana V, Tencomnao T. Rhinacanthus nasutus extracts prevent glutamate and amyloid-β neurotoxicity in HT-22 mouse hippocampal cells: possible active compounds include lupeol, stigmasterol and β-sitosterol. International journal of molecular sciences. 2012;13(4):5074-5097.
30. Wang Z, Park SH, Zhao H, Peng S, Zuo Z. A critical role of glutamate transporter type 3 in the learning and memory of mice. Neurobiology of learning and memory. 2014;114:70-80.
31. Cao J, Wang Z, Mi W, Zuo Z. Isoflurane unveils a critical role of glutamate transporter type 3 in regulating hippocampal GluR1 trafficking and context-related learning and memory in mice. Neuroscience. 2014;272:58-64.

32. Holmseth S, Dehnes Y, Huang YH, Follin-Arbelet VV, Grutle NJ, Mylonakou MN, et al. The density of EAAC1 (EAAT3) glutamate transporters expressed by neurons in the mammalian CNS. The Journal of neuroscience. 2012;32(17):6000-6013.
33. Lee S, Park SH, Zuo Z. Effects of isoflurane on learning and memory functions of wild-type and glutamate transporter type 3 knockout mice. The Journal of pharmacy and pharmacology. 2012;64(2):302-307.
34. Lee SN, Li L, Zuo Z. Glutamate transporter type 3 knockout mice have a decreased isoflurane requirement to induce loss of righting reflex. Neuroscience. 2010;171(3):788-793.
35. González LF, Henríquez-Belmar F, Delgado-Acevedo C, Cisternas-Olmedo M, Arriagada G, Sotomayor-Zárate R, et al. Neurochemical and behavioral characterization of neuronal glutamate transporter EAAT3 heterozygous mice. Biological research. 2017;50(1):29.
36. Van Zandt M, Weiss E, Almyasheva A, Lipior S, Maisel S, Naegele JR. Adeno-associated viral overexpression of neuroligin 2 in the mouse hippocampus enhances GABAergic synapses and impairs hippocampal-dependent behaviors. Behavioural brain research. 2019;362:7-20.
37. Jang M, Lee SE, Cho IH. Adeno-Associated Viral Vector Serotype DJ-Mediated Overexpression of N171-82Q-Mutant Huntingtin in the Striatum of Juvenile Mice Is a New Model for Huntington's Disease. Frontiers in cellular neuroscience. 2018;12:157.
38. Woldbye DP, Angehagen M, Gøtzsche CR, Elbrønd-Bek H, Sørensen AT, Christiansen SH, et al. Adeno-associated viral vector-induced overexpression of neuropeptide Y Y2 receptors in the hippocampus suppresses seizures. Brain. 2010;133(9):2778-2788.
39. Minami T, Matsumura S, Nishizawa M, Sasaguri Y, Hamanaka N, Ito S. Acute and late effects on induction of allodynia by acromelic acid, a mushroom poison related structurally to kainic acid. British journal of pharmacology. 2004;142(4):679-688.
40. Lewerenz J, Maher P. Chronic Glutamate Toxicity in Neurodegenerative Diseases-What is the Evidence? Frontiers in neuroscience. 2015;9:469.
41. Nieoullon A, Canolle B, Masmejean F, Guillet B, Pisano P, Lortet S. The neuronal excitatory amino acid transporter EAAC1/EAAT3: does it represent a major actor at the brain excitatory synapse? Journal of neurochemistry. 2006;98(4):1007-1018.
42. Underhill SM, Ingram SL, Ahmari SE, Veenstra-VanderWeele J, Amara SG. Neuronal excitatory amino acid transporter EAAT3: Emerging functions in health and disease. Neurochemistry international. 2019;123:69-76.
43. Potenza N, Mosca N, Mondola P, Damiano S, Russo A, De Felice B. Human miR-26a-5p regulates the glutamate transporter SLC1A1 (EAAT3) expression. Relevance in multiple sclerosis. Biochimica et biophysica acta Molecular basis of disease. 2018;1864(1):317-323.
44. Rumpel S, LeDoux J, Zador A, Malinow R. Postsynaptic receptor trafficking underlying a form of associative learning. Science. 2005;308(5718):83-88.
45. Man HY, Sekine-Aizawa Y, Huganir RL. Regulation of {alpha}-amino-3-hydroxy-5-methyl-4-isoxazolepropionic acid receptor trafficking through PKA phosphorylation of the Glu receptor 1

subunit. Proceedings of the National Academy of Sciences of the United States of America. 2007;104(9):3579-3584.

46. Whitlock JR, Heynen AJ, Shuler MG, Bear MF. Learning induces long-term potentiation in the hippocampus. Science. 2006;313(5790):1093-1097.
47. Esteban JA, Shi SH, Wilson C, Nuriya M, Huganir RL, Malinow R. PKA phosphorylation of AMPA receptor subunits controls synaptic trafficking underlying plasticity. Nature neuroscience. 2003;6(2):136-143.
48. Cao J, Tan H, Mi W, Zuo Z. Glutamate transporter type 3 regulates mouse hippocampal GluR1 trafficking. Biochimica et biophysica acta. 2014;1840(6):1640-1645.
49. Caffino L, Messa G, Fumagalli F. A single cocaine administration alters dendritic spine morphology and impairs glutamate receptor synaptic retention in the medial prefrontal cortex of adolescent rats. Neuropharmacology. 2018;140:209-216.
50. Borczyk M, Śliwińska MA, Caly A, Bernas T, Radwanska K. Neuronal plasticity affects correlation between the size of dendritic spine and its postsynaptic density. Scientific reports. 2019;9(1):1693.
51. Zhang JC, Wu J, Fujita Y, Yao W, Ren Q, Yang C, et al. Antidepressant effects of TrkB ligands on depression-like behavior and dendritic changes in mice after inflammation. The international journal of neuropsychopharmacology. 2014;18(4).
52. Zhao W, Xu Z, Cao J, Fu Q, Wu Y, Zhang X, et al. Elamipretide (SS-31) improves mitochondrial dysfunction, synaptic and memory impairment induced by lipopolysaccharide in mice. Journal of neuroinflammation. 2019;16(1):230.
53. Maysinger D, Gröger D, Lake A, Licha K, Weinhart M, Chang PK, et al. Dendritic Polyglycerol Sulfate Inhibits Microglial Activation and Reduces Hippocampal CA1 Dendritic Spine Morphology Deficits. Biomacromolecules. 2015;16(9):3073-3082.
54. Inoue H, Okada Y. Roles of volume-sensitive chloride channel in excitotoxic neuronal injury. The Journal of neuroscience. 2007;27(6):1445-1455.
55. Swiatkowski P, Nikolaeva I, Kumar G, Zucco A, Akum BF, Patel MV, et al. Role of Akt-independent mTORC1 and GSK3β signaling in sublethal NMDA-induced injury and the recovery of neuronal electrophysiology and survival. Scientific reports. 2017;7(1):1539.

Figures

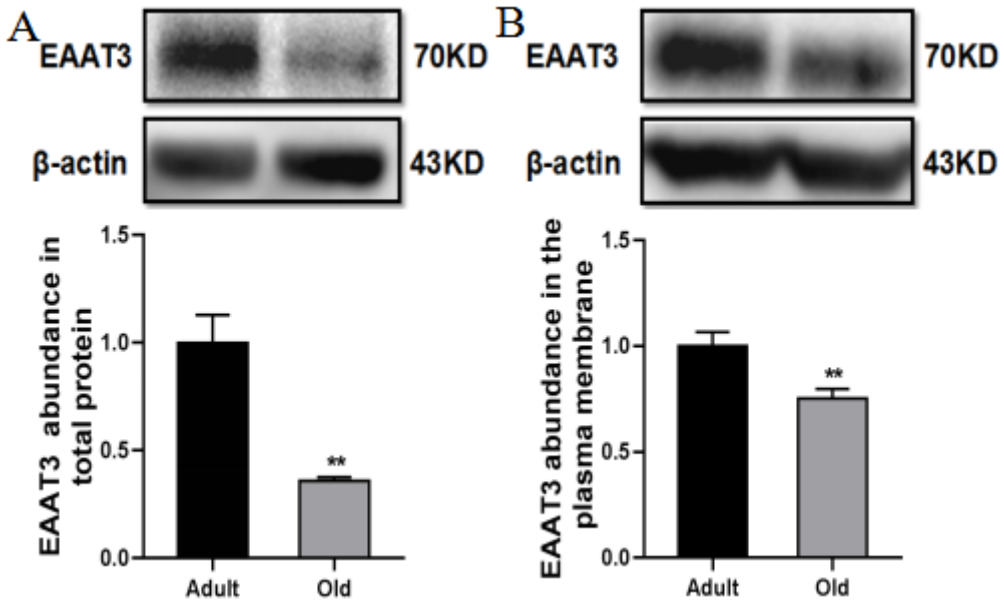

Figure 1

Expression of EAAT3 is different in different age mice. (A) EAAT3 expression of total protein in the hippocampus of old mice was significantly lower than that in adult mice. (B) EAAT3 expression of membrane protein in the hippocampus of old mice was significantly lower than that in adult mice. Data are expressed as mean ± SE (n= 6). **P <0.01.

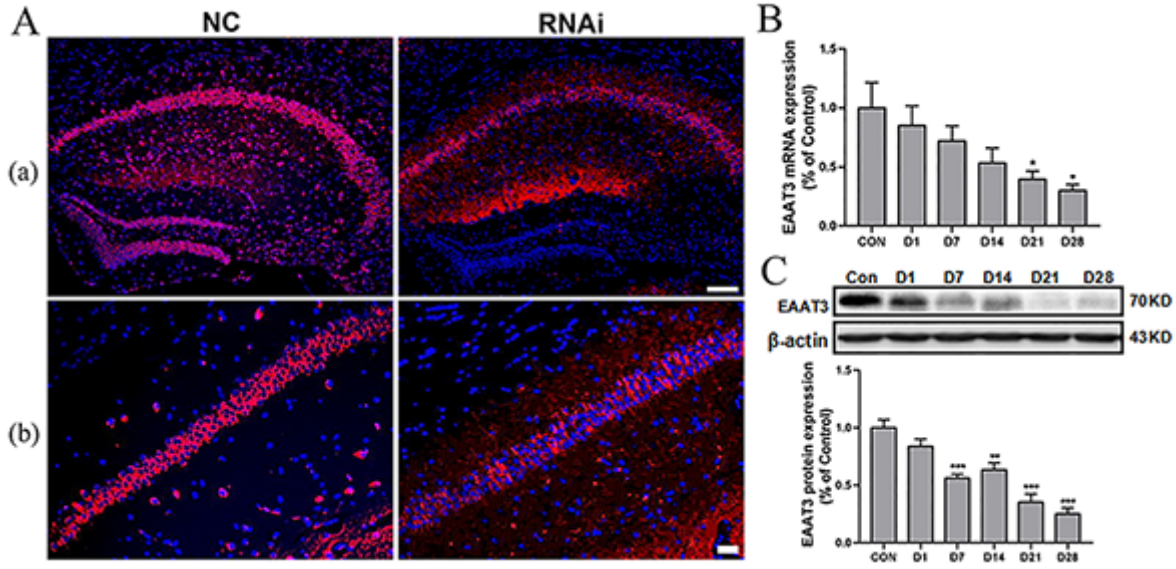

Figure 2

The expression of EAAT3 in the hippocampus of adult mice decreased after microinjection rAAV-RNAi. (A) Representative images of hippocampal EAAT3 expression 21 days after viral injection. EAAT3 protein expression in the whole hippocampus (Aa) and EAAT3 protein expression in the hippocampal CA regions (Ab). (B, C) Trends of EAAT3 relative expression in the hippocampus by mRNA (B) and western blot (C) after receiving virus injection. Data are expressed as mean ± SE (n=6). The scale bar in Figure Aa is 100 μm, and the scale bar in Figure Ab is 20μm. *P <0.05, **P <0.01, ***P <0.001, vs. control. CON

(immediately after microinjection of the hippocampus), control; D1, 7, 14, 21, 28 (1day, 7days, 14days, 21days, 28days after microinjection).

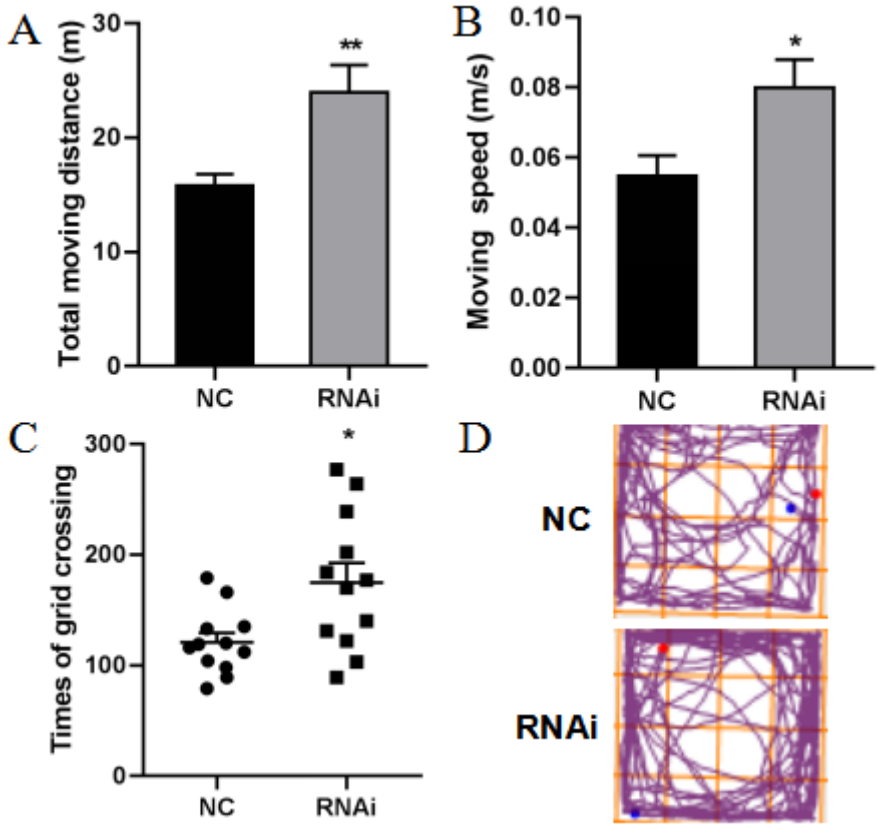

Figure 3

EAAT3 knockdown in the hippocampus increased motility of adult mice. (A-D) Total moving distance (A) and moving speed (B) are expressed as the mean ± SE; times of grid crossing (C) is expressed as median (first quartile, third quartile) (n=10); representative moving traces in the open arena (D). *P<0.05, **P<0.01.

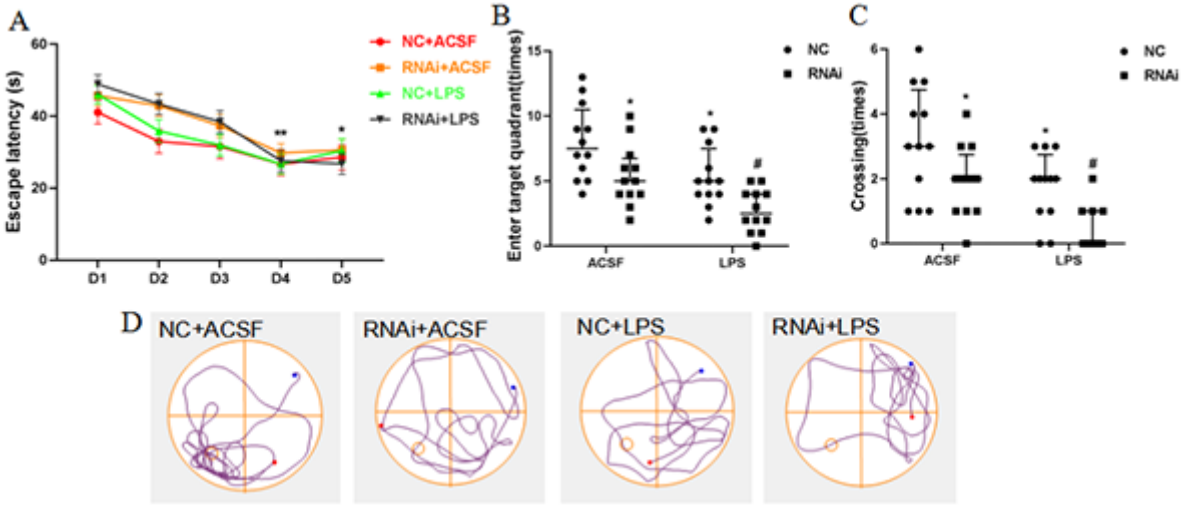

Figure 4

EAAT3 knockdown in the hippocampus aggravated LPS-induced learning and memory deficits in adult mice. (A) All experimental groups of mice learned to locate the hidden platform by using the surrounding cues after 5-day training. (B, C) During the probe trial, the hidden platform was removed; enter target quadrant (B), and platform-site crossings (C) were analyzed. (D) Representative trajectories of adult mice from each experimental group in probe trial, the circle represents the previous location of the platform. Data are expressed as median (first quartile, third quartile) (n=12). *P <0.05, vs. NC+ACSF group; #P <0.05, vs. NC+LPS group.

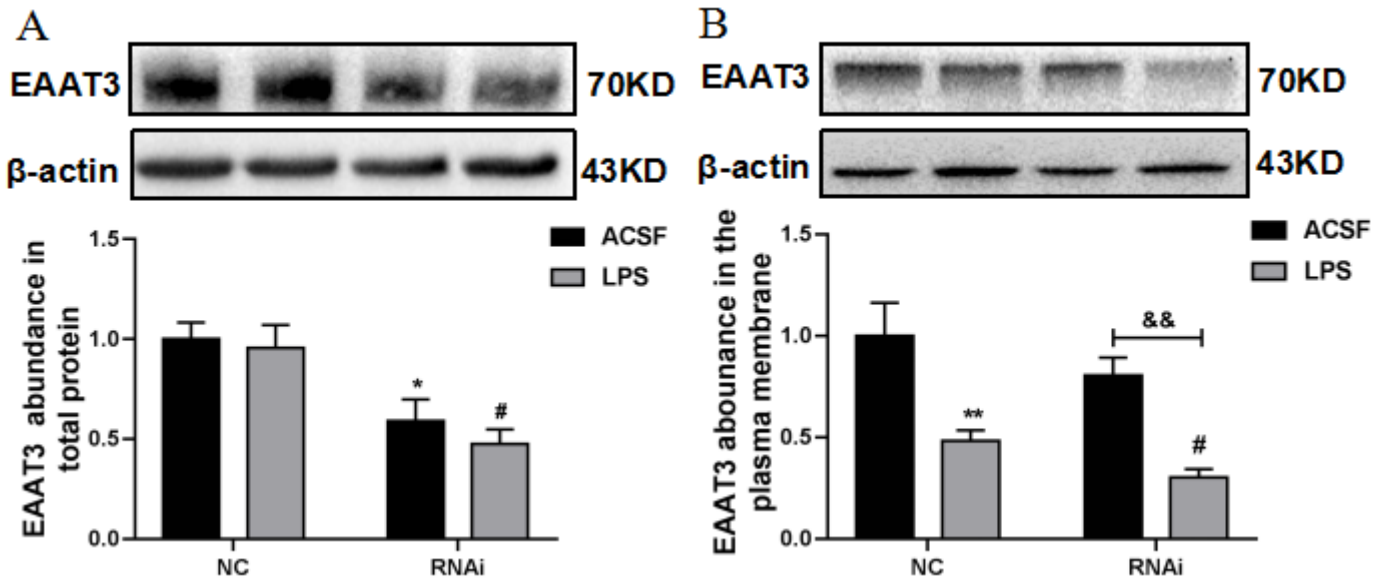

Figure 5

Effects of LPS lateral ventricle microinjection on hippocampus EAAT3 expression in the adult mice. (A, B) Protein bands on the gel and their relative intensities. The expression levels of EAAT3 protein in total protein and plasma membrane of the hippocampus in adult mice were normalized to that of β-actin as an internal control. Data are expressed as mean ± SE (n=6). *P <0.05, **P <0.01, vs. NC+ACSF group; #P <0.05, vs. NC+LPS group; &&P <0.01 vs. RNAi+ACSF group.

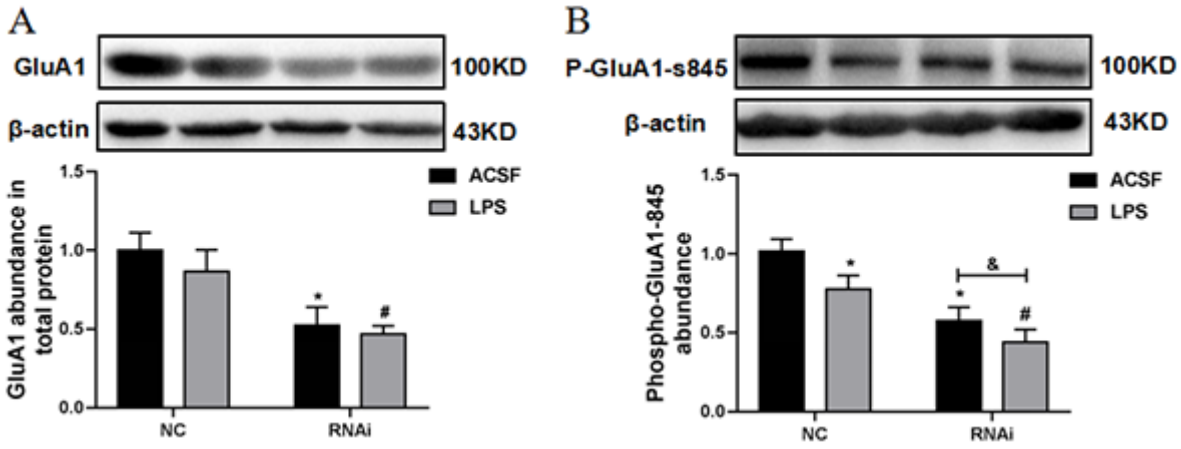

Figure 6

Expression of GluA1 proteins and GluA1 phosphorylation is inhibited by LPS-induced neuroinflammatory in the hippocampus of EAAT3 knockdown mice. (A, B) Protein bands on the gel and their relative intensities. The expression levels of GluA1 protein and Phospho-GluA1-Ser845 in the total protein of hippocampus were normalized to that of β-actin as an internal control. Data are expressed as mean ± SE (n=6). *P <0.05, vs. NC+ACSF group; #P <0.05, vs. NC+LPS group; &P <0.05, vs. RNAi+ACSF group.

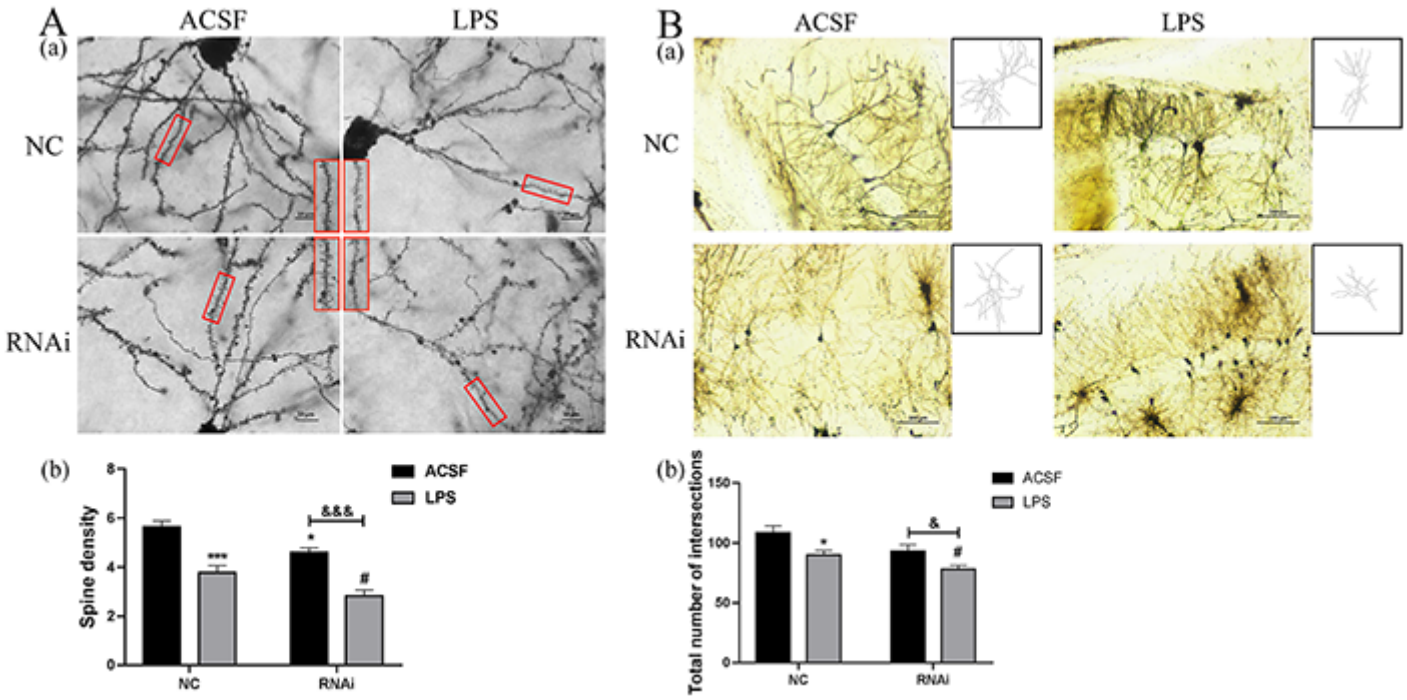

Figure 7

Effects of LPS on neuron dendritic morphogenesis in the hippocampus of EAAT3 dysfunctional mice. (A, B) The density of dendritic spines (Aa) and dendritic branch numbers (Ba) of the hippocampal neuron one day after LPS Intracerebroventricular injection was demonstrated by Golgi-Cox Staining. Data are expressed as mean ± SE (n=6). For the spine density (Ab), *P <0.05, ***P <0.001 vs. NC+ACSF group; #P <0.05 vs. NC+LPS group; &&&P <0.001 vs. RNAi+ACSF group. For the total number of intersection (Bb), *P <0.05 vs. NC+ACSF group; #P <0.05 vs. NC+LPS group; &P <0.05 vs. RNAi+ACSF group. The scale bar in Figure A is 10 μm, and the scale bar in Figure B is 100μm.

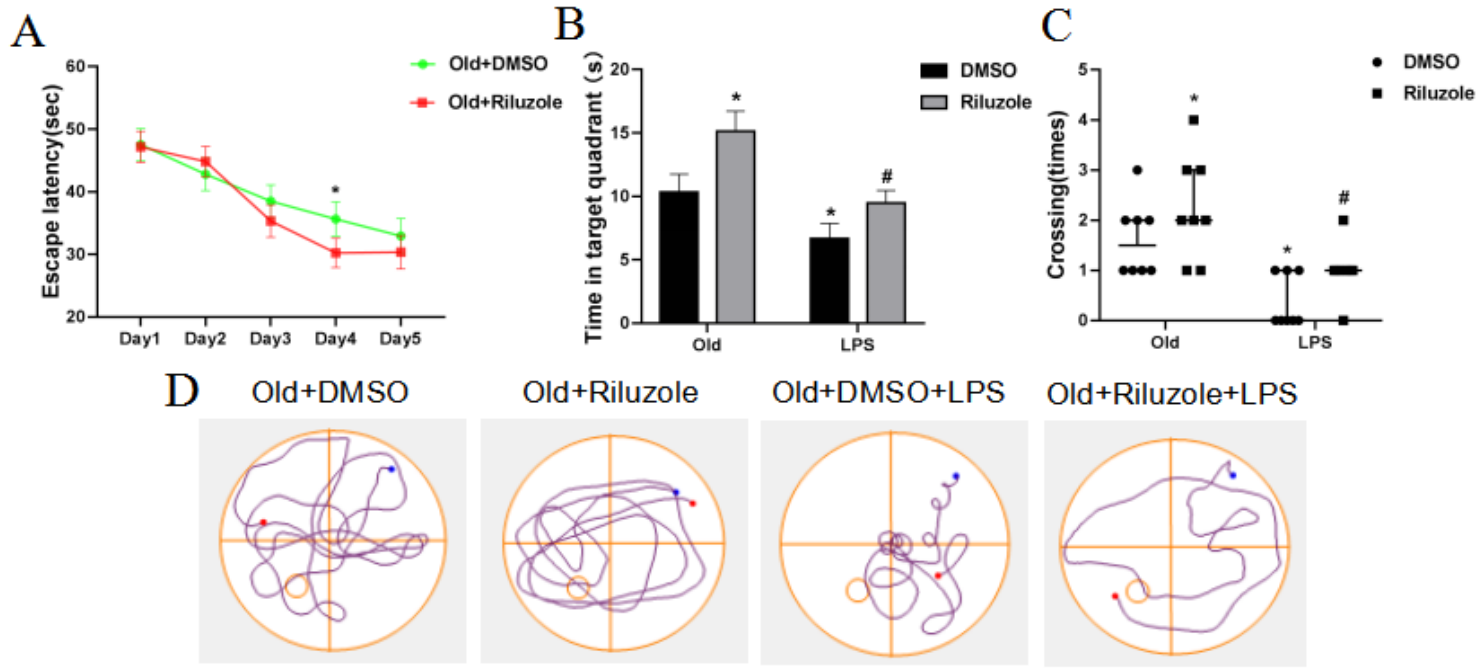

Figure 8

Riluzole improves learning and memory ability and LPS-induced cognitive impairment in old mice. (A, B) During the probe trial, the hidden platform was removed; time in target quadrant expressed as the mean ± SE (A), and platform-site crossings expressed as median (first quartile, third quartile) (B) were analyzed (n=8). (C) Representative trajectories of aged mice from each experimental group in probe trial, the circle represents the previous location of the platform. *P<0.05 vs. Old+DMSO group; #P<0.05, vs. Old+DMSO+LPS group.

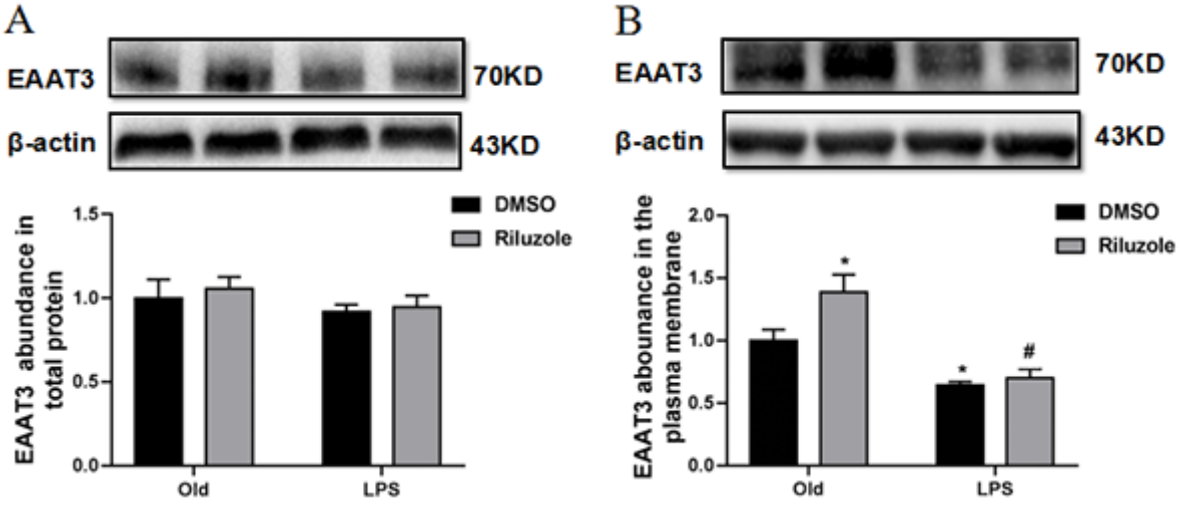

Figure 9

Riluzole increases the expression of EAAT3 in hippocampal membrane protein of old mice. (A, B) Protein bands on the gel and their relative intensities. The expression levels of EAAT3 protein in the total protein and plasma membrane of the hippocampus in aged mice were normalized to that of β-actin as an

internal control. Data are expressed as mean ± SE (n=4). *P<0.05, vs. Old+DMSO group; #P<0.05, vs. Old+Riluzole group.

Supplementary Files

This is a list of supplementary files associated with this preprint. Click to download.

- Supplementaryfigures.docx